New Journal of Physics
The open access journal at the forefront of physics

Deutsche Physikalische Gesellschaft DPG
IOP Institute of Physics

Published in partnership with: Deutsche Physikalische Gesellschaft and the Institute of Physics

OPEN ACCESS

RECEIVED
17 April 2018

REVISED
20 June 2018

ACCEPTED FOR PUBLICATION
29 June 2018

PUBLISHED
18 July 2018

PAPER

Wavelength-dispersive spectroscopy in the hard x-ray regime of a heavy highly-charged ion: the 1s Lamb shift in hydrogen-like gold

T Gassner[1,2], M Trassinelli[3], R Heß[2], U Spillmann[1,2], D Banaś[4], K-H Blumenhagen[1], F Bosch[2,16], C Brandau[2,5], W Chen[2], Chr Dimopoulou[2], E Förster[1,6], R E Grisenti[2,7], A Gumberidze[2,8], S Hagmann[2,7], P-M Hillenbrand[2], P Indelicato[9], P Jagodzinski[10], T Kämpfer[1], Chr Kozhuharov[2], M Lestinsky[2], D Liesen[2,11], Yu A Litvinov[2], R Loetzsch[1,6], B Manil[12], R Märtin[1], F Nolden[2], N Petridis[2,7], M S Sanjari[2], K S Schulze[1,6], M Schwemlein[1], A Simionovici[13], M Steck[2], Th Stöhlker[1,2,6], C I Szabo[9,14], S Trotsenko[1], I Uschmann[1,6], G Weber[1], O Wehrhan[1], N Winckler[2], D F A Winters[2], N Winters[2], E Ziegler[15] and H F Beyer[2]

[1] Helmholtz-Institut Jena, D-07743 Jena, Germany
[2] GSI Helmholtzzentrum für Schwerionenforschung, D-64291 Darmstadt, Germany
[3] Institut des NanoSciences de Paris, CNRS, Sorbonne Université, F-75005 Paris, France
[4] Institute of Physics, Jan Kochanowski University, 25406 Kielce, Poland
[5] Physikalisches Institut, Justus-Liebig-Universität Gießen, D-35392 Gießen, Germany
[6] Institut für Optik und Quantenelektronik, Friedrich-Schiller-Universität, D-07737 Jena, Germany
[7] Institut für Kernphysik, Goethe-Universität, D-60438 Frankfurt am Main, Germany
[8] ExtreMe Matter Institute EMMI and Research Division, GSI Helmholtzzentrum für Schwerionenforschung, D-64291 Darmstadt, Germany
[9] Laboratoire Kastler Brossel, Sorbonne Université, ENS-PSL Research University, Collège de France, CNRS, F-75005 Paris, France
[10] Department of Mathematics and Physics, Kielce University of Technology, 25-314 Kielce, Poland
[11] Fakultät für Physik und Astronomie, Ruprecht-Karls-Universität, D-69117 Heidelberg, Germany
[12] Laboratoire de Physique des Lasers, CNRS, Université Paris 13, F-93430 Villetaneuse, France
[13] Institut des Sciences de la Terre, UGA, CNRS, CS 40700, F-38058 Grenoble, France
[14] Theiss Research, 7411 Eads Ave, La Jolla, CA 92037, United States of America
[15] European Synchrotron Radiation Facility, F-38043 Grenoble, France
[16] Deceased 16.12.2016.

E-mail: martino.trassinelli@insp.jussieu.fr

Keywords: quantum electrodynamics test, strong Coulomb field, energy-dispersive x-ray spectroscopy, storage rings

Abstract

Accurate spectroscopy of highly-charged high-Z ions in a storage ring is demonstrated to be feasible by the use of specially adapted crystal optics. The method has been applied for the measurement of the 1s Lamb shift in hydrogen-like gold (Au^{+78}) in a storage ring through spectroscopy of the Lyman x-rays. This measurement represents the first result obtained for a high-Z element using high-resolution wavelength-dispersive spectroscopy in the hard x-ray regime, paving the way for sensitivity to higher-order QED effects.

1. Introduction

The theory of quantum electrodynamics (QED) has been tested for light atoms with extraordinarily high accuracy [1–6]. Yet, in the recent years, measurements on muonic hydrogen (combined with the state-of-the-art QED calculations), have produced inconsistency with the results obtained from hydrogen spectroscopy [7, 8]. The experimental verification of the QED predictions is still significantly less accurate in the domain of extreme field strength as experienced by an electron bound to a nucleus with high atomic number Z. In contrast to low-Z ions, bound state QED corrections for high-Z ions are still a challenge for theory since they have to be treated in all orders of αZ.

The QED corrections to the electronic binding energy, made up by the self energy and the vacuum polarization, are most important for the inner shells of high-Z systems since they approximately scale as Z^4/n^3 [9], where n denotes the principal quantum number. Hydrogen and hydrogen-like ions are the most fundamental atomic systems where the QED effects can be calculated with high accuracy, thus offering a

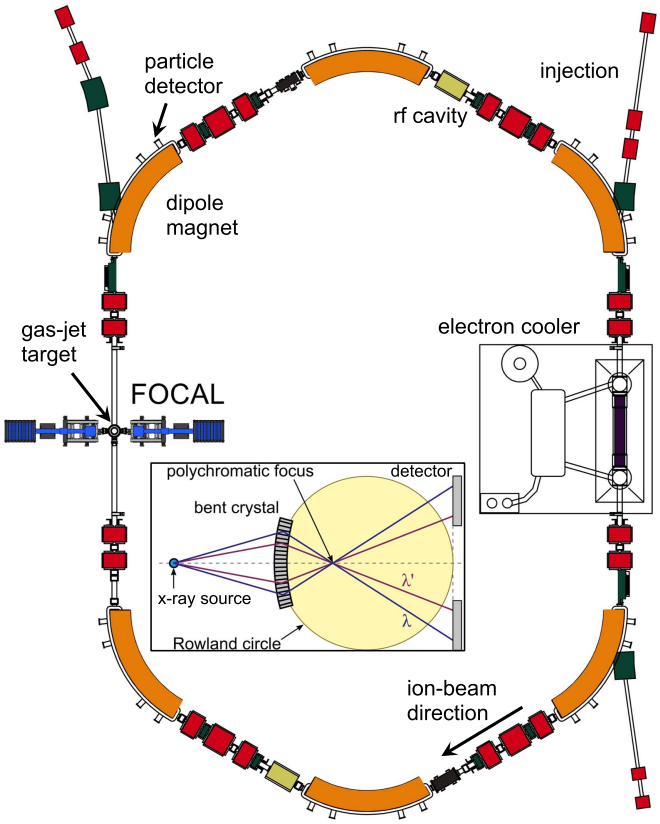

Figure 1. Schematic view of the ESR storage ring and the location of the FOCAL spectrometer at the gas-jet target. In the upper left dipole magnet a particle detector recording down-charged ions is used to apply a coincidence condition on the x-ray spectra. The inset shows a schematic view of the FOCAL crystal optics layout.

possibility of stringent experimental tests. From the experimental point of view it requires the preparation of heavy hydrogen-like ions where notably the 1*s* Lamb shift can be accessed via x-ray spectroscopy of an $np \rightarrow 1s$ Lyman transition from which the calculated Dirac energy plus the small QED contribution of the *np* level are subtracted. Such measurements have initially been performed at lower Z where ion intensities were sufficient for the use of high-resolution techniques with low detection efficiency [10–15]. With the advent of heavy-ion accelerators and storage rings as well as of new generation ion traps the investigations were extended to H-, He- and Li-like ions with highest nuclear charges up to $Z = 92$ [16–29].

However, in the case of the Lamb shift of the 1*s* level in high-Z H-like systems, where the strongest Coulomb fields can be obtained, the spectroscopy needed to be conducted with solid state Ge(i) detectors ensuring a high detection efficiency, although they soon faced their limits in spectral resolution. To circumvent the low resolving power of semiconductor detectors, they were replaced by specially adapted crystal spectrometers, as will be reported in this letter, and by calorimetric low-temperature detectors yielding promising results in first storage-ring experiments [30, 31]. In the present experiment a pair of crystal spectrometers was used to measure the 1s Lamb shift of hydrogen-like gold accomplishing for the first time both, high-Z ions and high spectral resolution. Envisioned for a long time, the measurements have become feasible only recently because of the following developments: (i) adapted and optimized crystal spectrometer optics, (ii) specially developed two-dimensionally position sensitive Ge(i) detectors for hard x-rays with both energy and time resolution and (iii) a substantial increase of the ion-beam intensity in the experimental storage ring (ESR) [32, 33].

2. Experimental setup

The experiment was performed at the accelerator and storage-ring facility of the GSI Helmholtz Centre for Heavy Ion Research in Darmstadt, Germany [34]. Up to 10^8 of fully ionized gold atoms ($^{197}Au^{79+}$) per pulse with an initial kinetic energy of about 300 MeV per nucleon were injected into the ESR (see figure 1). Here, they were stored, cooled, and decelerated to a final velocity of $\beta = v_{ion}/c = 0.471\,36(10)$. The relative momentum spread ($\Delta p/p$) of the cooled ion beam is typically in the range of 10^{-4}–10^{-5}. The cooled Au^{+79} ions were then brought into interaction with the ESR internal gas-target in the form of a supersonic gas-jet overlapping with the circulating ion beam. A typical gas area density of $\sim 10^{12}$ atoms cm^{-2} guaranteed single collision conditions and

a reasonably long ion beam storage time of several tens of seconds. In the present experiments, krypton has been used as target gas. During each collision one ion has a chance to capture an electron from the target atom into an excited state, which then decays either directly or in a very rapid cascade to the $1s$ ground state of the newly formed hydrogen-like ion. About $1/3$ of all down-charged ions decay (among other transitions in the cascade) via the Lyman-α_1 ($2p_{3/2} \rightarrow 1s$) transition, the accurate spectroscopy of which is the main goal of the present experiment.

The Lyman-α_1 transition wavelength is measured by a set of two identical spectrometers operated in the focussing compensated Laue (FOCAL) geometry [35, 36]. This type of spectrometer is well suited to find the right compromise between superior spectral resolving power and sufficient detection efficiency in the situation of very limited source strength and the presence of strong Doppler effects. Since the radiation source moves with relativistic velocity relative to the resting detector assembly (the laboratory frame) the velocity and observation angle dependent Doppler effect has to be taken into account. The wavelength λ_{Lab} observed in the laboratory frame at the angle θ is given by

$$\lambda_{\mathrm{Lab}} = \lambda_0 \gamma (1 - \beta \cos\theta), \tag{1}$$

where λ_0 is the rest-frame transition wavelength and $\gamma = 1/\sqrt{1-\beta^2}$ is the Lorentz factor. The velocity of the ion beam is set by the electron cooler, however it seems unfeasible to aim for a determination of the actual observation angle with comparable accuracy.

The two identical crystal spectrometer arms are aligned perpendicular with respect to the ion beam at both sides of the interaction chamber on one common line of sight. Both spectrometers are used to measure the Lyman-α_1 transition independently of each other leading to two distinct results for the wavelength $\lambda_{1,2}$. In this special geometry rest-frame transition wavelength λ_0 can be derived via

$$\lambda_1 + \lambda_2 = 2\,\gamma\,\lambda_0. \tag{2}$$

This geometry thus cancels out the uncertainty due to the observation angle stemming in particular from the possible misalignment of the beam.

The wavelengths $\lambda_{1,2}$ are measured with respect to a calibration line from an isotope enriched ^{169}Yb source. The strong and well known 63 120.44(4) eV γ transition [37] was selected as the main calibration line. The ion-beam velocity has been chosen such ($\beta = 0.471\,36(10)$), that the Doppler-shifted lab-frame energy of the Lyman-α_1 transition approximately coincides with this calibration energy thus avoiding systematic uncertainties due to large extrapolations. The wavelength comparison is made with respect to the dispersion plane defined by the crystals and detectors of the twin spectrometers.

The actual crystal optics layout of each FOCAL spectrometer arm is shown in the inset of figure 1. The emitted x-ray radiation is Bragg diffracted by the cylindrically bent silicon single crystal, with a bending radius of 2 m [35]. The diffracted x-rays cross the polychromatic focus and are recorded in one of the position sensitive x-ray detectors. Due to the curvature of the crystal, the spatially wide x-ray radiation is focused to a narrow line at the edge of the Rowland circle whose diameter is equal to the crystal bending radius. The intensity of x-rays emitted from the Au^{78+} reaction products is too faint in order to allow the usage of a conventional crystal spectrometer geometry. For this purpose an *asymmetric* crystal cut has been applied with an angle deviation of $\chi = 2°$ from the symmetric Laue case, where the reflecting lattice planes are orientated perpendicular with respect to the principal crystal faces. This asymmetric cut leads to a broadening of the crystal reflection curve, thereby enhancing the efficiency by more than a factor of 20 [35]. The bent crystal is rotated by the angle χ to correct for the asymmetric cut, leading to symmetric but mirrored reflections above and below the optical axis.

The position sensitive x-ray detectors are located close to the Rowland circle to make use of this focusing effect. Each spectrometer arm is equipped with one germanium microstrip detector consisting of an 11 mm thick germanium single crystal with both anode and cathode segmented into many strips [38] resulting in a quantum efficiency of 85% for 63 keV photons. The cathode is divided into 128 56 mm wide and 250 μm high strips, whereas the anode is segmented into 48 1.2 mm wide and 32 mm high strips. The strips on the front and on the back side are oriented perpendicularly with respect to each other allowing a two-dimensional position reconstruction if front and back side strips are combined for events with the same measured energy. The narrow strips on the front are orientated perpendicularly to the dispersive direction of the spectrometer allowing for a more accurate position determination.

Both spectrometers are passively shielded by 15 mm thick lead plates and several thick tungsten diaphragms along the ray path to ensure that the majority of the detected photons stem from a diffractive process from the crystal. Additional background suppression was achieved by active shielding making use of the fact that the down-charged ions follow a different trajectory in the bending dipole magnets of the ESR, where they were recorded by a particle detector [39] with efficiency close to 100%. X-ray events in the germanium detectors have been taken into account only if a singly down-charged ion has been coincidentally detected in the particle detector.

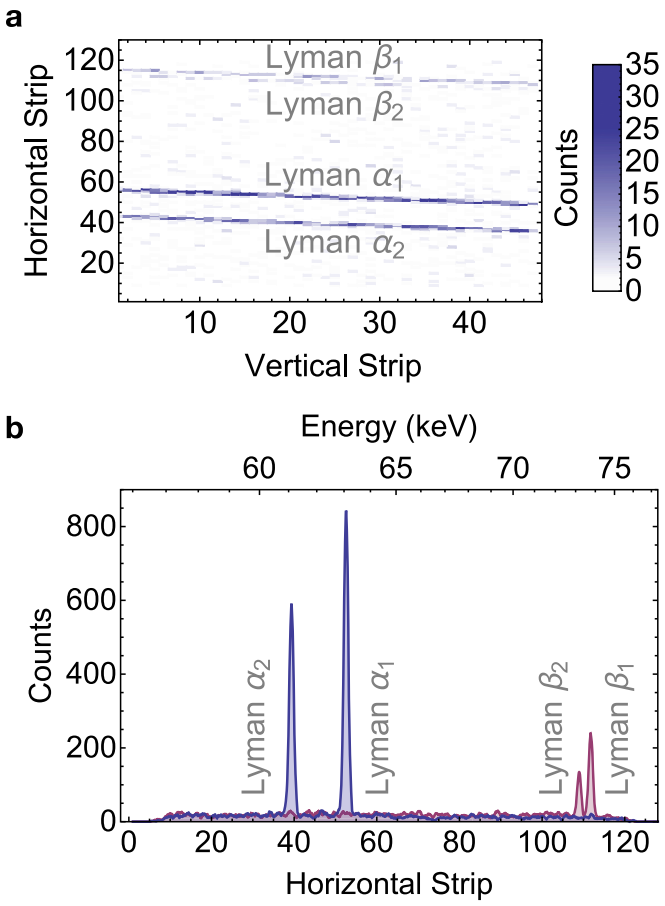

Figure 2. (a) Coincident x-ray spectrum as recorded by one of the FOCAL spectrometers. (b) Spectrum of the Lyman-α (blue curve) and -β (red curve) doublets of Au^{78+} obtained by projections of the respective two-dimensional intensity distribution shown in (a).

3. Results

Figure 2(a) shows the Lyman spectrum of H-like gold as measured by one of the two spectrometers by applying appropriate energy and time coincidence conditions to the data. In this way almost background free lines are revealed as can be seen in the figure. In a period of three weeks, about 1500 Lyman-α_1 photons per spectrometer arm could be collected, almost without interruptions. The event rate for this line was about 3.5 counts per hour. This low rate is principally due to the low transmission of the spectrometer of 3×10^{-8} [36]. In addition to the Lyman-α, also the spatially resolved Lyman-β transitions could be recorded, clearly evidencing the high resolving power of FOCAL. The slight tilt of the lines over several horizontal strips is caused by an effect called Doppler slanting. Due to the spatial extent of the 2D detector a certain observation angle interval is covered, leading to higher Doppler shifted (laboratory frame) transition energies in forward angles relative to the backward direction. Figure 2(b) shows the spectrum obtained by projection of the 2D image in figure 2(a) according to the tilt angle.

Since the spectrometer is operated as a wavelength comparator only the relative distance Δz_d between the main ^{169}Yb-γ calibration line and the Lyman-α_1 line matters. This distance was determined by fitting a 2D model function to the original (not projected) measurement data for the Lyman and the ^{169}Yb calibration data. The fitting results can be found in table 1. Here the minus sign indicates that the measured laboratory frame energy lies below the ^{169}Yb-γ line energy. Possible model dependencies and details of the line shape have also been addressed [36] by applying various fitting procedures resulting in negligible uncertainties.

Besides the line spacing also the spectrometers dispersion D for both assemblies has to be measured. This was done by fitting in addition to the main ^{169}Yb-γ calibration line, the thulium K$\beta_{1,3}$ transitions, which are present in the calibration source spectra. The results are listed in table 1.

By using equation (2), we thus obtain a preliminary Lyman-α_1 transition energy of $E^{\text{prel.}}_{\text{Ly-}\alpha_1} = 71\ 539.8(2.2)$ eV, which does not include any systematic effects so far.

Table 1. Line spacing between the main ^{169}Yb-γ calibration line and the Lyman-α_1 transition, and the measured spectrometer dispersion.

	Δz_d (μm)	Spectrometer dispersion
FOCAL 1	−35.2(5.1)	$1.905\,29(53) \times 10^{-10}$
FOCAL 2	−51.8(3.6)	$1.909\,74(52) \times 10^{-10}$

Table 2. Individual contributions to the total Lyman-α_1 transition energy.

Contribution	Value (eV)
Preliminary transition energy	71 539.8(2.2)
Temporal drift	–(2.8)
Gas-target position	+3.2(13.0)
Ion-beam velocity	–(4.3)
Detector-crystal position	−11.6(5.1)
Total	71 531.5(15.0)

4. Systematic effects and uncertainties

The systematic effects do not only increase the total uncertainty but may also shift the final value of the Lyman-α_1 transition energy. All possible contributions are discussed below and are listed in table 2 with the corresponding estimated uncertainties.

The first systematic effect was the temporal drift of the assembly during the three weeks of beam time. The drifts were monitored by the ^{169}Yb calibrations which were done every six hours. In total it was less than 100 μm for both spectrometers. With the help of the numerous calibrations the effect could be minimized, adding $\pm$2.8 eV to the total uncertainty.

If the ion beam is misaligned or it is shifted along the common line of sight between the two spectrometer arms, the FOCAL geometry corrects for that effect. However, if the source position (i.e. ion-beam–gas-target intersection region) is shifted out of that line (i.e. along the ion beam direction) this misalignment cannot be corrected leading to a systematic deviation. For the actual position measurement of the gas-jet target a dedicated auxiliary experiment was performed in the aftermath of the beam time [40] and the position of the gas-jet target was measured with an uncertainty of $\pm$0.30 mm revealing an offset of 0.25 mm in the ion beam direction. The corrected gas-jet position represents our present best guess. However, because of the long time which has passed between the main and the auxiliary experiment, we need to increase the position uncertainty to $\pm$1 mm in order to account for possible long time changes (due to mechanical manipulations, venting and pumping, etc). Fluctuations of this magnitude have previously been observed when checking the optical alignment of the gas-jet nozzles or when measuring the maximum overlap of the ion beam with the gas-jet. For the Lyman α_1 transition energy it means a correction of 3.2 eV with an associated uncertainty of $\pm$13 eV.

Also the uncertainty in the ion-beam velocity has to be considered, which is mainly caused by an insufficiently accurate calibration of the high-voltage terminal of the electron cooler. Another correction to be added is due to the space charge of the electron beam. Details concerning the evaluation of these corrections and the associated uncertainties can be found in [41–43]. The influence on the total uncertainty of this systematic effect is $\pm$4.3 eV.

The last and strongest influence on the final value is given by the actual position of the germanium detector crystal inside the housing of the position sensitive x-ray detector. For its measurement, a dedicated beam time at the European Synchrotron Radiation Facility (ESRF) in Grenoble, France, has been conducted where an intense and narrow x-ray beam can be provided. The position sensitive detector was mounted on a movable table directly facing the x-ray beam. In small steps the detector was moved and the count rate of the strips as a function of the detector position was recorded. The location of the germanium crystal was thus measured relative to the outer fiducial marks, which were also used during the original experimental assembly. The findings from the ESRF measurement lead to a systematic energy decrease of 11.6 eV with an uncertainty of $\pm$5.1 eV.

Our final experimental value for the Lyman-α_1 transition energy including all statistical and systematic uncertainties (added quadratically) is given by $E^{\mathrm{exp.}}_{\mathrm{Ly\text{-}}\alpha_1} = 71\,531.5(15.0)$ eV.

Table 3. The 1*s* Lamb shift of Au^{78+} in eV.

Present experiment	244.1(15.0)
Beyer *et al* 1995 [44]	202.3(7.9)
Kraft-Bermuth *et al* 2016 [30]	211(42)
Theory, Yerokhin and Shabaev 2015 [9]	205.2(2)

5. Lamb shift evaluation and discussions

The experimental value for the 1*s* Lamb shift is obtained by subtracting the FOCAL value for the Lyman-α_1 transition energy from the theoretical value for the $2p_{3/2}$ binding energy, which is sufficiently well known [9]. The difference between this value and the Dirac value for the 1*s* binding energy yields the 1*s* Lamb shift. With the theoretical value for the $2p_{3/2}$ binding energy $E^{\text{theo.}}_{2p_{3/2}} = -21\,684.201(5)$ eV one obtains $\Delta E^{\text{exp.}}_{1s} = 244.1(15.0)$ eV. In table 3 our result is compared to the experimental value obtained with a Ge(i) detector in an early experiment at the ESR electron cooler [44] and to the experimental result reported for the calorimetric low-temperature detectors which was obtained in the same beam time [30] as our present experiment. In the last entry of table 3 the theoretical value of Yerokhin and Shabaev [9] is given. Our present value of the Lamb shift is higher than the theoretical value and the other experimental results by about 2.5 standard deviations of the estimated experimental uncertainty.

It is difficult at this stage to unambiguously pinpoint the reasons for this deviation. Without going into details of the other results which would be beyond the scope of this article, it should be stated that these measurements have all been performed with different techniques, i.e. semiconductor detector at the electron cooler [44], microcalorimeter at the gas-jet target [30] and thus are prone to different systematic effects. It is important to emphasize that even though we have performed very thorough and extensive studies of the various possible systematic effects, since this is the first measurement of its kind at the storage ring, potentially underestimated or unknown systematic effects cannot be fully excluded. Therefore more measurements are required in order to clarify this issue.

6. Conclusions

In conclusion we performed a first measurement of the ground state Lamb shift in a heavy H-like ion (Au^{78+}) using a high resolution crystal spectrometer in combination with a fast and dim source of hard x-rays as present at a heavy-ion storage ring. The energy resolution corresponding to about 60 eV FWHM at 63 keV photon energy [36] surpasses the best semiconductor detectors by almost one order of magnitude. The achieved statistical uncertainty of 2.2 eV is groundbreaking for a crystal spectrometer operated in the region of hard x-rays of H-like high-*Z* ions. Since storage rings are currently the only facilities routinely delivering high-*Z* hydrogen-like ions in large quantities, this measurement represents a very important milestone towards the challenging goal of achieving a sensitivity to higher-order QED effects as it is planned at the FAIR facility [45]. In a future run, particular effort has to be put into avoiding or reducing systematic uncertainties. The ion-beam velocity can already be determined with a much higher accuracy using a high-voltage divider from the Physikalisch-Technische Bundesanstalt in the electron cooler terminal, which will establish an absolutely calibrated velocity standard [46]. With a slightly modified assembly it will also be possible to measure the gas-target position relative to the detector-crystal position *in situ*, which will almost entirely eliminate these systematic uncertainties avoiding supplementary experiments altogether.

Furthermore, we would like to emphasize that this apparatus can also be applied for precision spectroscopy of heaviest helium-like ions (as well as other few-electron systems) which, taking into account the unprecedented resolution, would allow for resolving all the relevant fine structure levels for the first time. This is especially interesting in the light of the recent controversy with the comparison between the experimental and theoretical results for helium-like ions [47–54].

Acknowledgments

Laboratoire Kastler Brossel (LKB) is 'Unité Mixte de Recherche de Sorbonne University-UPMC, de ENS-PSL Research University, du Collège de France et du CNRS n° 8552'. Institut des NanoSciences de Paris (INSP) is 'Unité Mixte de Recherche de Sorbonne University-UPMC et du CNRS n° 7588'. This work has been partially supported by: the European Community FP7—Capacities, contract ENSAR n° 262010, the Allianz Program of the Helmholtz Association contract n° EMMI HA-216 "Extremes of Density and Temperature: Cosmic Matter

in the Laboratory", the Helmholtz-CAS Joint Research Group HCJRG-108 and by the German Ministry of Education and Research (BMBF) under contract 05P15RGFAA.

ORCID iDs

M Trassinelli https://orcid.org/0000-0003-4414-1801
P-M Hillenbrand https://orcid.org/0000-0003-0166-2666
Yu A Litvinov https://orcid.org/0000-0002-7043-4993
M S Sanjari https://orcid.org/0000-0001-7321-0429

References

[1] Fee M S, Chu S, Mills A P, Chichester R J, Zuckerman D M, Shaw E D and Danzmann K 1993 *Phys. Rev.* A **48** 192–219
[2] van Wijngaarden A, Holuj F and Drake G W F 2000 *Phys. Rev.* A **63** 012505
[3] Karshenboim S G 2005 *Phys. Rep.* **422** 1–63
[4] Parthey C G *et al* 2011 *Phys. Rev. Lett.* **107** 203001
[5] Cancio Pastor P, Consolino L, Giusfredi G, De Natale P, Inguscio M, Yerokhin V A and Pachucki K 2012 *Phys. Rev. Lett.* **108** 143001
[6] Notermans R and Vassen W 2014 *Phys. Rev. Lett.* **112** 253002
[7] Pohl R *et al* 2010 *Nature* **466** 213–6
[8] Antognini A *et al* 2013 *Science* **339** 417–20
[9] Yerokhin V A and Shabaev V M 2015 *J. Phys. Chem. Ref. Data* **44** 033103
[10] Briand J P, Tavernier M, Indelicato P, Marrus R and Gould H 1983 *Phys. Rev. Lett.* **50** 832
[11] Briand J P, Mossé J P, Indelicato P, Chevallier P, Girard-Vernhet D, Chetioui A, Ramos M T and Desclaux J P 1983 *Phys. Rev.* A **28** 1413–7
[12] Briand J P, Indelicato P, Tavernier M, Gorceix O, Liesen D, Beyer H F, Liu B, Warczak A and Desclaux J P 1984 *Z. Phys.* A **318** 1–5
[13] Richard P, Stockli M, Deslattes R, Cowan P, LaVilla R, Johnson B, Jones K, Meron M, Mann R and Schartner K 1984 *Phys. Rev.* A **29** 2939–42
[14] Beyer H F, Deslattes R D, Folkmann F and LaVilla R E 1985 *J. Phys. B: At. Mol. Phys.* **18** 207–15
[15] Beyer H F, Indelicato P, Finlayson K D, Liesen D and Deslattes R D 1991 *Phys. Rev.* A **43** 223
[16] Munger C T and Gould H 1986 *Phys. Rev. Lett.* **57** 2927
[17] Martin S, Buchet J P, Buchet-Poulizac M C, Denis A, Désesquelles J, Druetta M, Grandin J P, Hennecart D, Husson X and Lecler D 1989 *Europhys. Lett.* **10** 645
[18] Briand J P *et al* 1989 *Europhys. Lett.* **9** 225
[19] Briand J P, Chevallier P, Indelicato P, Ziock K P and Dietrich D D 1990 *Phys. Rev. Lett.* **65** 2761–4
[20] Indelicato P, Birkett B B, Briand J P, Charles P, Dietrich D D, Marrus R and Simionovici A 1992 *Phys. Rev. Lett.* **68** 1307
[21] Beiersdorfer P, Knapp D, Marrs R E, Elliott S R and Chen M H 1993 *Phys. Rev. Lett.* **71** 3939
[22] Lupton J H, Dietrich D D, Hailey C J, Stewart R E and Ziock K P 1994 *Phys. Rev.* A **50** 2150–4
[23] Crespo López-Urrutia J R, Beiersdorfer P, Savin D W and Widmann K 1996 *Phys. Rev. Lett.* **77** 826–9
[24] Crespo López-Urrutia J R, Beiersdorfer P, Widmann K, Birkett B B, Mårtensson-Pendrill A M and Gustavsson M G H 1998 *Phys. Rev.* A **57** 879–87
[25] Beiersdorfer P, Osterheld A L, Scofield J H, Crespo López-Urrutia J R and Widmann K 1998 *Phys. Rev. Lett.* **80** 3022
[26] Bosselmann P, Staude U, Horn D, Schartner K H, Folkmann F, Livingston A E and Mokler P H 1999 *Phys. Rev.* A **59** 1874–83
[27] Stöhlker T *et al* 2000 *Phys. Rev. Lett.* **85** 3109–12
[28] Gumberidze A *et al* 2005 *Phys. Rev. Lett.* **94** 223001
[29] Beiersdorfer P, Chen H, Thorn D B and Trabert E 2005 *Phys. Rev. Lett.* **95** 233003
[30] Kraft-Bermuth S *et al* 2017 *J. Phys. B: At. Mol. Opt. Phys.* **50** 055603
[31] Hengstler D *et al* 2015 *Phys. Scr.* **2015** 014054
[32] Beyer H *et al* 2004 *Spectrochim. Acta* B **59** 1535–42
[33] Chatterjee S *et al* 2006 *Nucl. Instrum. Methods Phys. Res., Sect.* B **245** 67–71
[34] Blasche K and Bohne D 1989 Status report on the GSI synchrotron facility and first beam results *Proc. 1989 IEEE Particle Accelerator Conf., 1989. Accelerator Science and Technology* vol 1, pp 27–8
[35] Beyer H F *et al* 2009 *Spectrochim. Acta* B **64** 736–43
[36] Beyer H F *et al* 2015 *J. Phys. B: At. Mol. Opt. Phys.* **48** 144010
[37] Bé M M, Chisté V, Dulieu C, Browne E, Chechev V, Kuzmenko N, Helmer R, Nichols A, Schönfeld E and Dersch R 2004 *Table of Radionuclides, (Monographie BIPM-5 Vol 2)* (France: Bureau International des Poids et Mesures)
[38] Spillmann U, Bräuning H, Hess S, Beyer H, Stöhlker T, Dousse J C, Protic D and Krings T 2008 *Rev. Sci. Instrum.* **79** 083101
[39] Klepper O and Kozhuharov C 2003 *Nucl. Instrum. Methods Phys. Res., Sect.* B **204** 553
[40] Gassner T and Beyer H F 2015 *Phys. Scr.* **2015** 014052
[41] Lochmann M 2013 Laserspektroskopie der Grundzustands-Hyperfeinstruktur des lithiumähnlichen $^{209}Bi^{80+}$ *PhD Thesis* Johannes Gutenberg-Universität Mainz
[42] Lochmann M *et al* 2014 *Phys. Rev.* A **90** 030501
[43] Brandau C 2000 Messungen zur Photorekombination hochgeladener lithiumähnlicher *PhD Thesis* Justus-Liebig-Universität Gießen
[44] Beyer H *et al* 1995 *Z. Phys.* D **35** 169–75
[45] Stöhlker T *et al* 2015 *Nucl. Instrum. Methods Phys. Res., Sect.* B **365** 680–5
[46] Hällström J *et al* 2014 *IEEE Trans. Instrum. Meas.* **63** 2264–70
[47] Trassinelli M *et al* 2009 *Europhys. Lett.* **87** 63001
[48] Chantler C T *et al* 2012 *Phys. Rev. Lett.* **109** 153001
[49] Amaro P, Schlesser S, Guerra M, Bigot E O L, Isac J M, Travers P, Santos J P, Szabo C I, Gumberidze A and Indelicato P 2012 *Phys. Rev. Lett.* **109** 043005
[50] Rudolph J K *et al* 2013 *Phys. Rev. Lett.* **111** 103002

[51] Kubiček K, Mokler P H, Mäckel V, Ullrich J and Crespo López-Urrutia J R 2014 *Phys. Rev.* A **90** 032508
[52] Payne A T, Chantler C T, Kinnane M N, Gillaspy J D, Hudson L T, Smale L F, Henins A, Kimpton J A and Takacs E 2014 *J. Phys. B: At. Mol. Opt. Phys.* **47** 185001
[53] Epp S W *et al* 2015 *Phys. Rev.* A **92** 020502
[54] Beiersdorfer P and Brown G V 2015 *Phys. Rev.* A **91** 032514